

# SEASONAL AND SPATIAL VARIABILITY OF OZONE INFERRED FROM GLOBAL CHEMISTRY TRANSPORT MODEL SIMULATIONS OVER INDIA

Yesobu Yarragunta<sup>1,2,\*</sup>, Shuchita Srivastava<sup>1</sup>, D. Mitra<sup>1</sup>, H.C. Chandola<sup>2</sup>

<sup>1</sup>Indian Institute of Remote Sensing, ISRO, Dehradun, India-(yesobu, shuchita, mitra)@iirs.gov.in

<sup>2</sup>Department of Physics, Kumaun University, Nainital, India- chandolaharish@gmail.com

Commission V, SS: Atmosphere, Ocean, Weather and Climate

**KEY WORDS:** Ozone, MOZART-4, Seasonal cycle, Spatial distribution, and seasonal maxima

## ABSTRACT:

In the present study, 3-D chemical transport model, MOZART-4 (Model for Ozone and Related chemical Tracers-Version-4) has been used to study the seasonal and spatial distribution of surface ozone (O<sub>3</sub>) over India. To illustrate the capabilities of model, the simulations are compared with the ground-based observations. The model reproduces the principal features present in ground-based observations. However, model is unable to simulate very low concentration of O<sub>3</sub> during monsoon months. The model simulations are used to quantify the contribution of background ozone and Indian anthropogenic emissions to the variability of surface O<sub>3</sub>. The spatial distribution of total O<sub>3</sub> (TO) shows maximum over Indo-Gangetic plains (IGP) and Eastern India while minimum over southern Indian region. The seasonal cycle of TO vary from 34.2±7.6 – 51.9±4.9 ppbv over the Indian landmass region due to changes in its topography and ozone lifetime. Annual mean total background O<sub>3</sub> (TBO) over India shows highest during spring (29.3±5.0 ppbv) and lowest during monsoon (19.6±3.4 ppbv). Both Natural background O<sub>3</sub> (NBO) and pollution background O<sub>3</sub> (PBO) shows a minimum in summer which are essentially following the seasonal changes of total ozone. Significant variation of India pollution O<sub>3</sub> (IPO) is found over India and the spatial variation of IPO follows the spatial variation of TO as well as spatial variation of emission of ozone precursors.

## 1. INTRODUCTION

The third most important anthropogenic greenhouse gas is the tropospheric O<sub>3</sub> after carbon dioxide (CO<sub>2</sub>) and methane (CH<sub>4</sub>) (Ehhalt and Prather, 2001) which plays a crucial role in the earth's radiation budget (Gauss, 2003). Higher concentration of O<sub>3</sub> in the atmospheric boundary layer may adversely affecting vegetation, animals as well as humans (Adams et al., 1989). Ozone is produced by rapid photochemical reactions of CO (carbon monoxide) and VOCs (volatile organic compounds) with OH (hydroxyl) radical in the presence of NO<sub>x</sub> (nitrogen oxides) and sunlight. Apart from this, downward transport of stratospheric O<sub>3</sub> into the troposphere is another source of the tropospheric O<sub>3</sub>. The contribution of later is much smaller on an annual and global scale, but it can be accountable in the regions of subsidence (Cooper et al., 2002). Anthropogenic activities (such as combustion of biofuel and fossil fuel), biomass burning, biogenic sources, and lightnings are the major sources of O<sub>3</sub> precursor gases like CO, NO<sub>x</sub>, and VOCs, etc. in the atmosphere. During later half of the 20<sup>th</sup> century, the fast economic growth and rapid industrialization of the developing countries has led to a dramatic increase in emission of these gases in the atmosphere. This subsequently lead to increase in ozone concentration in the lower troposphere (Wang et al., 2006; Roy et al., 2008; Kim et al., 2013).

Thus, tropospheric O<sub>3</sub> and its precursor gases play a crucial role in the degradation of air quality, atmospheric chemistry, and climate change (e.g. Stevenson et al., 2013; WHO, 2003; Monks et al., 2015). In recent years, numerous in-situ ground-based measurements (Lal et al., 2000; Kumar et al., 2010) and very few ship-based campaigns (Srivastava et al., 2012 references therein) have been initiated to account the spatio-temporal variation of O<sub>3</sub> and precursors over Indian

region. However, most of these measurements are confined to the specific region and for short durations. These in-situ observations are unable to explain the different atmospheric processes accountable for high pollution events. Therefore, chemistry transport models are valuable for providing a large-scale view of the regional impact of these gases and are useful for interpretation of observations on regional to global scale (Yarragunta et al., 2017). In the present work, in-situ observations have been used to understand the variability of O<sub>3</sub> over the Indian subcontinent and to evaluate the chemistry transport model, MOZART-4. The MOZART-4 model simulations are used to investigate seasonal and spatial variation of surface ozone as well as to identify the contribution of various sources (natural and anthropogenic) and its horizontal distribution over the Indian sub-continent. Along with seasonal analysis of ozone is also presented over different geographical regions of India.

## 2. METHODOLOGY

### 2.1 The Model for Ozone and Related chemical Tracers-Version-4

The global chemistry transport model, MOZART-4 (Model for Ozone and Related chemical Tracers-Version-4) which is jointly developed by the NCAR (National Center for Atmospheric Research), GFDL (NOAA Geophysical Fluid Dynamics Laboratory) and MPI-Met (Max Planck Institute for Meteorology). MOZART-4 contained comprehensive tropospheric chemistry which includes more than 130 chemical and aerosol species and 157 chemical reactions (Emmons et al., 2010). MOZART-4 is driven by assimilated meteorological data from the GEOS-5 (Goddard Earth Observing System version 5) of the NASA Global Modelling and Assimilation Office (<https://www.earthsystemgrid.org/dataset/ucar.cgd.ccsm4.g>

\* Corresponding author

eos5.html) with a temporal resolution of 6 hours for 2007-2008. The MOZART-4 outputs have been saved daily from 01 July 2006 to 31 December 2008 and first 6 months of simulated data have been considered as spin up time (01 July 2006 – 31 December 2006). The model horizontal resolution has 1.9° latitude by 2.5° longitude and simulated up to 2 hPa, with 56 sigma-pressure levels. The POET (Precursors of Ozone and their Effects in the Troposphere) anthropogenic emissions of different chemical species included in the present work for 2000. These emissions have been updated with the Regional Emission inventory in Asia (REAS) inventory over South Asia (Ohara *et al.*, 2007). The emissions from biomass burning have been provided from Global Fire Emissions Database version-2 (GFED-2) on monthly basis (van der Werf *et al.*, 2006). Emissions of isoprene and monoterpenes from vegetation are also included based on the online calculations of the MEGAN (Model of Emissions of Gases and Aerosols from Nature) [Guenther *et al.*, 2006]. Emmons *et al.*, (2010) is provided the full description about MOZART-4 model.

## 2.2 Model simulations

The simulation with emissions described above is treated as standard simulation. Two sensitivity simulations are also performed in which simulation 1 corresponds to all anthropogenic emissions of NO<sub>x</sub> (Oxides of nitrogen), CO and non-methane hydrocarbons are removed with in Indian region, simulation 2 corresponds to the simulation 1 but are removed these emissions globally. The sensitivity simulation 1 gives ozone concentration levels that would exist in the absence of Indian anthropogenic emissions which is represented as total background ozone (TBO) over India. Sensitivity simulation 2 gives natural background ozone (NBO) over India, while the difference between these two sensitivity simulations represent pollution background ozone (PBO) or the enhanced ozone due to anthropogenic emissions outside the India. The differences between standard simulation and sensitivity simulation 1 are attributed to the ozone enhancement due to anthropogenic emissions of India, considered as Indian pollution ozone (IPO). The IPO for the present day may be higher than what reported in the present study which used emissions of 2008. These simulations are summarized in table 1 and the modelling approach follows the concept of Fiore *et al.*, (2002) and Wang *et al.*, (2011). The standard model results are compared with ground-based observations by linearly interpolating the model output to the geographical locations of observational sites. The evaluation of O<sub>3</sub> would reveal the strengths and weakness in the model on the temporal and seasonal scales.

Name	Description
1. Standard simulation	Anthropogenic and natural emissions as described in the text (Sect. 2.1)
2. Indian total background ozone	Same as 1 but without the Indian anthropogenic emissions
3. Natural background	Same as 1 but without the global anthropogenic emissions

Table 1 MOZART-4 simulations used in the present study

## 3. RESULTS AND DISCUSSION

### 3.1 Comparison with ground-based observations

In order to find the performance of model in case of seasonal cycle, the comparison of monthly observed and simulated mixing ratios of O<sub>3</sub> have been compared in the follow section. The monthly distribution of O<sub>3</sub> have been reported in different observational sites over Indian region. The details of each site viz. latitude, longitude, elevation, period of study and reference are given in Table 2 and the geographical location of each site is shown in Fig. 1(a). The monthly distribution of O<sub>3</sub> mixing ratio has been taken from the following observational sites viz. Anantapur (14.7N, 77.6E) (Ahammed *et al.*, 2006), Ahmedabad (23.0N, 72.6E) (Sahu and Lal, 2006), Delhi (28.6N, 77.2E) (Jain *et al.*, 2005), Hyderabad (17.4N, 78.5E) (Surendran *et al.*, 2015), Nainital (29.2N, 79.3 E) (Kumar *et al.*, 2010), Pune (18.5N, 73.9E) (Beig *et al.*, 2007), Kanpur (26.5N, 80.3E) (Gaur *et al.*, 2014), Mount Abu (24.6N, 72.7E) (Naja *et al.*, 2003), Chennai (13.1N, 80.4E) (Surendran *et al.*, 2015), and Udaipur (24.6N, 73.7E) (Yadav *et al.*, 2014). Fig. 2 represent the comparison of monthly mean observed surface O<sub>3</sub> mixing ratios with monthly simulated results at above said locations. Generally, model reproduced the observed seasonal cycle reasonably well over all measurement sites except Delhi, Kanpur, and Nainital where model fails to capture the minimum concentration of O<sub>3</sub> during monsoon months. Over Chennai, the systematic overestimation of O<sub>3</sub> mixing ratio by the model has been found throughout the year. The simulated O<sub>3</sub> mixing ratio showed maxima during spring over all the measurement sites except Delhi and Chennai where this feature is not clearly evident. The observed surface concentration of O<sub>3</sub> is between 7 ppbv and 60 ppbv whereas the simulated O<sub>3</sub> is between 27 ppbv and 53 ppbv among these observational sites. The observed O<sub>3</sub> is maximum during spring and minimum during summer over urban sites (Delhi, Kanpur, Ahmedabad, Udaipur, Chennai, and Hyderabad). The model is unable to reproduce this minimum concentration during summer. The observed O<sub>3</sub> mixing ratio over Nainital and Mount Abu is maximum during late spring and late autumn respectively. The simulated O<sub>3</sub> mixing ratio is maximum during late spring and spring/autumn respectively. Their range of absolute difference is -9.6 - 20.5 ppbv and -13.0– 10.8 ppbv respectively. Anantapur and Pune showed maximum observed O<sub>3</sub> mixing ratio during spring and minimum during monsoon months while simulated mixing ratio peaks during autumn and dips during the monsoon period. The quantitative difference is maximum during autumn and minimum during monsoon season over both the sites.

These observed seasonal changes are attributed to the changing wind pattern. Westerly winds during pre-monsoon and south-westerly or south-easterly winds during summer monsoon season prevail over Indian region. The strong westerly winds during pre-monsoon season bring pollution rich air masses to the observational sites resulting in higher levels of O<sub>3</sub> and its precursor gases. The higher observed O<sub>3</sub> mixing ratios during pre-monsoon season are also due to photochemical transformation, long-range transport of air pollutants (Lal *et al.*, 2013; Kumar *et al.*, 2010a) and atmospheric boundary layer dynamics (Lal *et al.*, 2000). South-westerly or south-easterly winds during summer-monsoon bring marine air from the oceanic regions (Guttikunda, 2010). The cleaner air from marine regions reduce the pollutant concentration in the continental air. In addition, insufficient sunshine for photochemical ozone

production, reduced impact of local emissions due to pronounced washout effect and strong convective activities are responsible for the minimum concentration of ozone in summer monsoon. The overall seasonality of ozone has been reproduced by model fairly well over all the sites. Improper representation of meteorological phenomenon, photochemical production, underestimation of dry deposition and wet scavenging of ozone precursors are some possible reasons of the overestimation of the observed O<sub>3</sub> concentration by the model. In addition, the local emissions are diluted in large grid boxes in the model due to its coarser resolution. These results are consistent with results presented by previous studies (Kumar et al., 2012; Surendran et al., 2015).

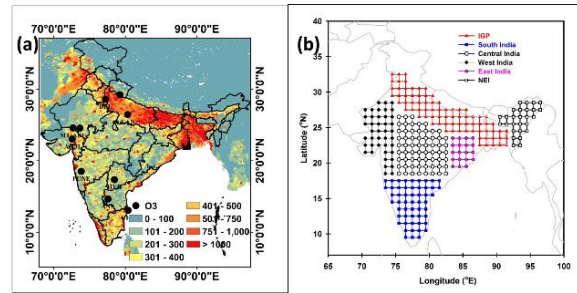


Fig. 1(a) Distribution of population density (people/km<sup>2</sup>) along with geographical locations of surface O<sub>3</sub> (circle) observational sites in India. b) Spatial division of Indian landmass region into the Indo-Gangetic Plain (IGP), Southern-India (SI), Central-India (CI), Western-India(WI), Eastern-India(EI), and North-Eastern India (NEI)

S. No.	Name	Lat.	Lon.	Elevation (m)	Site Type	Period of Study	Reference
1	Anantapur (ANA)	14.7	77.6	331	Rural	2001-03	Ahmed et al., 2006
2	Ahmedabad (AHM)	23.0	72.6	49	Urban	2002	Sahu & Lal, 2006
3	Delhi (DEL)	28.6	77.2	220	Urban	1997-03	Jain et al., 2005
4	Hyderabad (HYD)	17.4	78.5	542	Urban	2010-13	Surendran et al., 2015
5	Nainital (NAI)	29.2	79.3	1958	High Altitude	2006-08	Kumar et al., 2010
6	Pune (PUNE)	18.5	73.9	559	Semi-Urban	2003-04	Beig et al., 2007
7	Kanpur (KAN)	26.5	80.3	125	Urban	2009-13	Gaur et al., 2014
8	Mount Abu (MT. ABU)	24.6	72.7	1680	High Altitude	1993-00	Naja et al., 2003
9	Chennai (CHE)	13.1	80.4	7	Urban	2010-13	Surendran et al., 2015
10	Udaipur (UDA)	24.6	73.7	598	Urban	2010-11	Yadav et al., 2014

Table 2. Monthly mean mixing ratios of ozone (ppbv) surface based observational sites are used for comparison in the present study.

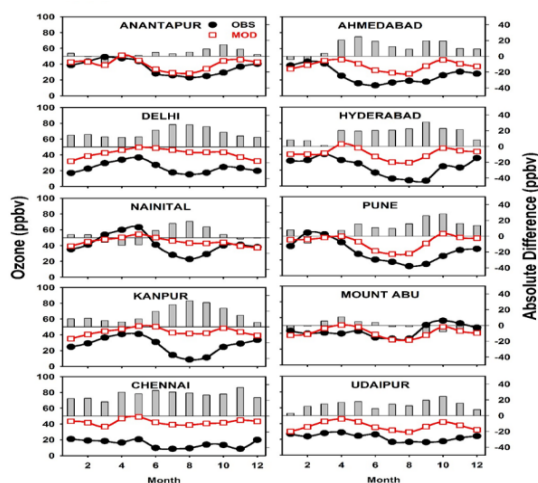


Fig. 2 Comparison of monthly averaged observed (black) and MOZART-4 simulated (red) surface O<sub>3</sub> mixing ratios at 10 surface based measurement sites. Vertical grey bar in Figure shows absolute difference between simulated and observed O<sub>3</sub>. Positive values represents model values higher than the observations and vice versa.

### 3.2 Contributions of surface ozone from MOZART

The previous analysis established the confidence over model simulations. The model is able to simulating the key features of surface ozone over India. The model sensitivity simulations introduced in the section 2.2 can be used to quantify the contributions of background and anthropogenic emissions to the total ozone on the seasonal scale over Indian landmass region. Table 3 summarizes the mean and spatial variability (defined as the standard deviation of all model grids with in the region) of surface ozone over India as a whole by season. The annual mean of TO over India is 43.3±6.7 ppbv, with minimum in summer (35.3±7.8 ppbv) and maximum in spring (50.1±6.7 ppbv). The annual mean TBO over India is 24.6±4.3 ppbv which accounts 57% of total surface ozone. The TBO is maximum (29.3±5.0 ppbv) in spring and minimum (19.6±3.4 ppbv) in summer, accounting for 57% and 56% of surface ozone in these seasons respectively. In all the seasons, more than 50% of total surface ozone is from TBO while at least 70 % of total background ozone is of natural origin except spring where it is only 53 %. The annual mean NBO is 17.5±3.6 ppbv which ranges from 14.9±2.8 ppbv in summer to 20.1±3.5 ppbv in winter. The IPO ranges from 15.7±5.8 to 20.8±5.2 ppbv which follows the seasonal pattern of TO.

Season	TO	TBO	NBO	IPO	PBO
Winter	43.3±5.4	25.4±4.3	20.1±3.5	17.9±4.7	5.3±2.8
Spring	50.1±6.7	29.3±5.0	15.5±4.3	20.8±5.2	13.8±2.5
Summer	35.3±7.8	19.6±3.4	14.9±2.8	15.7±5.8	4.7±2.0
Autumn	44.6±6.6	24.2±4.4	19.3±3.7	20.4±4.7	4.9±2.2
Annual	43.3±6.7	24.6±4.3	17.5±3.6	18.7±5.1	7.2±2.4

Table 3. Surface ozone and its decomposition (TO: total surface ozone, TBO: total background ozone, NBO: natural background ozone, IPO: Indian Pollution ozone (IPO) and PBO: pollution background ozone) averaged over India by season. Results are presented as mean ± spatial variability (unit: ppbv).

### 3.2.1 Ozone spatial distributions

The annual and spring mean variation of total ozone concentration, contribution coming from various sources are shown in the Fig. 3 and Fig.4 respectively. The annual mean total surface ozone concentration shows large spatial variability over India.

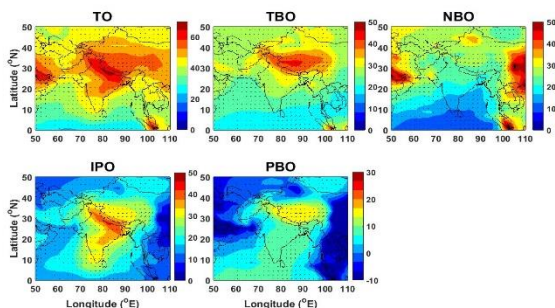


Fig. 3 Annual mean spatial distribution of surface ozone (ppbv) over India. This figure shows that the total surface ozone (TO), total background ozone (TBO), natural background ozone (NBO), Indian Pollution ozone (IPO) and pollution background ozone (PBO) for the year 2008. Horizontal surface wind vectors from the National Centers for Environmental Prediction/National Center for Atmospheric Research (NCEP/NCAR) re-analysis are overlaid on each plot.

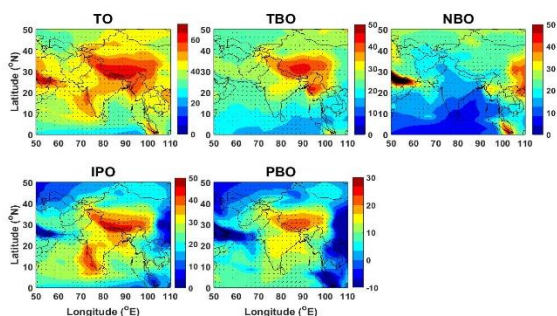


Fig. 4 Same as Fig.3 but for spring (March-May) season mean concentration of surface ozone over Indian region.

The total surface ozone over IGP and Eastern part of India shows approximately 60 to 70 ppbv whereas Central India shows 50 to 60 ppbv. The western India and southern India shows comparatively less total surface ozone of 40 to 50 ppbv. One of the strong reasons behind the high ozone episode over IGP and central India is increasing population (Fig.1 (a)) which enhance the human activities in the recent

years. The clean marine air influx dilutes the polluted air over the southern part of India. The TBO has been less in the southern part around 10 to 20 ppbv. The IPO shows high surface ozone concentration over IGP and eastern part of India. The similar variation of TO and its decompositions are found during spring season. However, the magnitude of the ozone is estimated differently. The TO is estimated as 15.7 % higher during spring as compared to annually estimated TO while TBO, NBO, IPO and PBO are estimated as 19.1 %, 11.4%, 33.6 % and 91.7 % respectively higher than those estimated annually over Indian region.

### 3.2.2 Ozone seasonality

After the spatial contribution analysis, the efforts has been made to study the seasonal mean surface ozone contribution over five different landmass regions of India. The seasonal contribution of surface ozone is analysed after interpolated MOZART simulations from a resolution of  $1.9^\circ \times 2.5^\circ$  to the  $1^\circ \times 1^\circ$  grid cell size. The Indian landmass subdivided into the five sub regions namely; Indo-Gangetic Plain (IGP), South-India (SI), Central-India (CI), West-India (WI), East-India (EI), and North-East India (NEI) which are shown in Fig. 1(b). The NEI is the most affected region by the biomass burning and fire events in the spring season. The IGP region is the major contributor of the ozone precursor's sources (CO, NO<sub>x</sub>, and NMHC's) due to the increasing anthropogenic emission activities in the recent years which is also known as area of high population density (Fig. 1(a)). The CI is also affected by the biomass burning events in the summer season due to the crop residue burning in the agricultural land.

The annual contribution of surface ozone concentration over six different regions given in the Table 4. The TO concentration is high over IGP region ( $49.0 \pm 7.0$  ppbv) while low over WI region ( $38.9 \pm 3.2$  ppbv). The IPO contribution is high over IGP (43%) while low over NEI (37%). The TBO concentration is high over IGP region ( $27.7 \pm 4.4$  ppbv) and NEI ( $27.4 \pm 3.7$  ppbv) while low over SI region ( $21.6 \pm 1.6$  ppbv). The Indian Pollution Ozone (IPO) gives the surface ozone concentration due to their own local anthropogenic emissions. The Indo-Gangetic plain and eastern India more affected by the ozone pollution.

Region	TO	TBO	NBO	IPO	PBO
India	43.3±6.7	24.6±4.3	17.5±3.6	18.7±5.1	7.2±2.4
IGP	49.0±7.0	27.7±4.4	19.7±3.0	21.3±5.0	8.1±2.2
WI	38.9±3.2	22.2±1.3	18.2±1.8	16.7±3.1	4.0±1.8
EI	45.6±2.5	24.8±1.1	17.0±0.9	20.8±1.7	7.8±0.5
NEI	43.7±3.8	27.4±3.7	19.7±3.1	16.3±3.0	7.7±1.8
CI	41.7±2.8	23.9±1.4	16.9±1.2	17.8±2.6	7.0±1.0
SI	39.6±3.6	21.6±1.6	13.4±1.6	18.0±2.8	8.2±0.8

Table 4. Annual average of total surface ozone (TO), total background ozone (TBO), natural background ozone (NBO), Indian Pollution ozone (IPO) and pollution background ozone (PBO) over different regions of India. Results are presented as mean ± spatial variability (unit: ppbv).

Fig. 5 shows the seasonal cycle of TO, TBO, IPO, NBO and PBO over different geographical regions defined in Fig. 1(a). In India, the estimated TO concentration is found to be high in the spring season ( $50.1 \pm 6.7$  ppbv) while low in the summer season ( $35.5 \pm 7.8$  ppbv). The IPO concentration high in the spring season ( $20.8 \pm 5.2$  ppbv) while low in the



summer season ( $15.7 \pm 5.8$  ppbv). The TBO and PBO also shows high during spring and low during summer while NBO shows high during winter season ( $20.1 \pm 3.5$  ppbv) while low in the summer season ( $14.9 \pm 2.8$  ppbv).

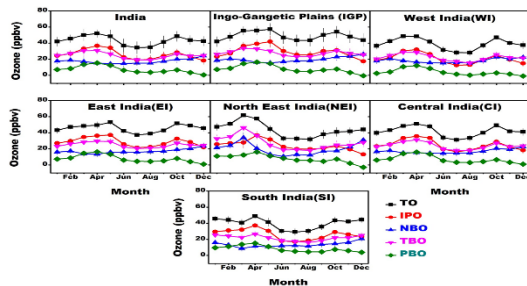


Fig. 5 Monthly variations of mean surface ozone (TO), total background ozone (TBO.), natural background ozone (NBO), pollution background ozone (PBO), and India pollution ozone (IPO) for different Indian regions defined in Fig. 1(b). Results are presented as mean  $\pm$  spatial variability (unit: ppbv).

Except NBO, all the components of ozone and TO are high during spring and low during summer. Table 5 shows the average surface concentration of ozone and its decomposed components during spring, 2008. TO, IPO and PBO shows maxima during spring over IGP while TBO and NBO shows maxima over NEI. The NBO contributes 63% to the TBO over NEI region where the forests are mainly sub-tropical evergreen with secondary successional fallow forests dominated by Bamboos. The NEI is the easternmost region of India and consists the seven hilly states of Meghalaya, Manipur, Arunachal Pradesh, Nagaland, Tripura, Mizoram and Assam. More than 4, 00,000 families practice slash and burn agriculture annually for cultivation during March-May which is just before the monsoon (Vadrevu et. al., 2013).

Region	TO	TBO	NBO	IPO	PBO
India	50.1 $\pm$ 6.7	29.3 $\pm$ 5.0	15.5 $\pm$ 4.3	20.8 $\pm$ 5.2	13.8 $\pm$ 2.5
IGP	56.1 $\pm$ 6.1	32.2 $\pm$ 3.6	16.9 $\pm$ 2.2	23.9 $\pm$ 5.5	15.3 $\pm$ 2.6
WI	46.2 $\pm$ 2.6	27.1 $\pm$ 1.1	16.6 $\pm$ 1.7	19.1 $\pm$ 3.2	10.4 $\pm$ 2.4
EI	50.3 $\pm$ 3.5	28.9 $\pm$ 1.8	14.3 $\pm$ 1.5	21.4 $\pm$ 2.1	14.7 $\pm$ 0.5
NEI	54.6 $\pm$ 2.7	35.6 $\pm$ 3.3	22.4 $\pm$ 4.4	19.0 $\pm$ 5.1	13.2 $\pm$ 2.3
CI	49.1 $\pm$ 2.4	29.4 $\pm$ 1.6	14.9 $\pm$ 1.3	19.7 $\pm$ 1.8	14.5 $\pm$ 1.2
SI	43.6 $\pm$ 4.0	23.7 $\pm$ 2.6	10.4 $\pm$ 2.2	19.9 $\pm$ 2.8	13.3 $\pm$ 0.9

Table 5. Average surface ozone and its decomposition (TO: total surface ozone, TBO: total background ozone, NBO: natural background ozone, IPO: Indian Pollution ozone (IPO) and PBO: pollution background ozone) averaged over different regions of India during spring (Mar-Apr-May). Results are presented as mean  $\pm$  spatial variability (unit: ppbv).

#### 4. CONCLUSIONS

Daily simulations of tropospheric O<sub>3</sub> have been made using MOZART-4 during 2008. The model simulated O<sub>3</sub> concentrations are evaluated against ground-based observations. The comparison of model results with in-situ observations at ten surface sites revealed that the model successfully reproduced the observed seasonal cycle at these observational sites. The magnitude of observed O<sub>3</sub> is in the range of 7 – 60 ppbv whereas the magnitude of simulated O<sub>3</sub> is in the range of 27– 53 ppbv. The high quantitative

difference of O<sub>3</sub> is estimated over Delhi, Hyderabad, Kanpur and Nainital during monsoon season but it is estimated differently over remaining observational sites. Model systematically overestimates observed O<sub>3</sub> over different observational sites during various seasons.

The contributions of various source types (natural and anthropogenic) to the seasonal distribution of surface ozone have been studied using global chemistry transport model, MOZART-4. The annual mean of TO over India is 43.3 $\pm$ 6.7 ppbv, with minimum in summer and maximum in spring. Annually 57% of total ozone is from TBO over India. The TBO is maximum during spring and minimum during summer, accounting 57% and 56% of surface ozone in these seasons respectively. In all the seasons, more than 50% of total surface ozone is from TBO while at least 70 % of total background ozone is of natural origin except spring where it is only 53 %. The IPO ranges from 15.7 $\pm$ 5.8 to 20.8 $\pm$ 5.2 ppbv which follows the seasonal pattern of TO. Spatial distribution of surface ozone shows approximately 60 to 70 ppbv over IGP and Eastern part of India whereas Central India shows 50 to 60 ppbv. The western and southern India shows minimum total surface ozone of 40 to 50 ppbv. Ozone seasonality shows that, except NBO, all the components of ozone and total ozone to be high during spring and low during summer. TO, IPO and PBO shows maxima during spring over IGP while TBO and NBO shows maxima over NEI during spring.

#### ACKNOWLEDGEMENT

The present research work was supported by the ISRO-Geosphere Biosphere Program under grant E3Z1701TF501. We are grateful to Director IIRS and Dean IIRS for their encouragement & support.

#### REFERENCES

- Adams, R. M., J. D. Glycer, S. L. Johnson, and B. a. McCarl (1989), A Reassessment of the Economic Effects of Ozone on U.S. Agriculture, JAPCA, 39(7), 960–968, doi:10.1080/08940630.1989.10466583.
- Ahammed, Y. N., R. R. Reddy, K. R. Gopal, K. Narasimhulu, D. B. Basha, L. S. S. Reddy, and T. V. R. Rao (2006), Seasonal variation of the surface ozone and its precursor gases during 2001-2003, measured at Anantapur (14.62°N), a semi-arid site in India, Atmos. Res., 80(2–3), 151–164, doi:10.1016/j.atmosres.2005.07.002.
- Beig, G., S. Gunthe, and D. B. Jadhav (2007), Simultaneous measurements of ozone and its precursors on a diurnal scale at a semi urban site in India, J. Atmos. Chem., 57(3), 239–253, doi:10.1007/s10874-007-9068-8.
- Cooper, O. R., J. L. Moody, D. D. Parrish, M. Trainer, T. B. Ryerson, J. S. Holloway, G. Hubler, F. C. Fehsenfeld, and M. J. Evans (2002), Trace gas composition of midlatitude cyclones over the western North Atlantic Ocean: A conceptual model, , 107, doi:10.1029/2001JD000901.
- Ehhalt, D., and M. Prather (2001), Atmospheric Chemistry and Greenhouse Gases, Clim. Chang. 2001 Sci. Basis, 239–287, doi:10.2753/JES1097-203X330403.
- Emmons, L. K. et al. (2010), Description and evaluation of

- the Model for Ozone and Related chemical Tracers, version 4 (MOZART-4), *Geosci. Model Dev.*, 3(1), 43–67, doi:10.5194/gmd-3-43-2010.
- Fiore, A. M., D. J. Jacob, I. Bey, R. M. Yantosca, B. D. Field, A. C. Fusco, and J. G. Wilkinson (2002), Background ozone over the United States in summer: Origin, trend, and contribution to pollution episodes, , 107.
- Gaur, A., S. N. Tripathi, V. P. Kanawade, V. Tare, and S. P. Shukla (2014), Four-year measurements of trace gases (SO<sub>2</sub>, NO<sub>x</sub>, CO, and O<sub>3</sub>) at an urban location, Kanpur, in Northern India, *J. Atmos. Chem.*, 71(4), 283–301, doi:10.1007/s10874-014-9295-8.
- Gauss, M. (2003), Radiative forcing in the 21st century due to ozone changes in the troposphere and the lower stratosphere, *J. Geophys. Res.*, 108(D9), 4292, doi:10.1029/2002JD002624.
- Guenther, a., T. Karl, P. Harley, C. Wiedinmyer, P. I. Palmer, and C. Geron (2006), Estimates of global terrestrial isoprene emissions using MEGAN (Model of Emissions of Gases and Aerosols from Nature), *Atmos. Chem. Phys. Discuss.*, 6(1), 107–173, doi:10.5194/acpd-6-107-2006.
- Guttikunda, S. (2010), Role of Meteorology on Urban Air Pollution Dispersion: A 20yr Analysis for Delhi, India, SIM-air Work. Pap. Ser. 31-2010.
- Jain, S. L., B. C. Arya, A. Kumar, S. D. Ghude, and P. S. Kulkarni (2005), Observational study of surface ozone at New Delhi, India, *Int. J. Remote Sens.*, 26(16), 3515–3524, doi:10.1080/01431160500076616.
- Kim, P. S., D. J. Jacob, X. Liu, J. X. Warner, K. Yang, K. Chance, V. Thouret, and P. Nedelec (2013), Global ozone–CO correlations from OMI and AIRS: constraints on tropospheric ozone sources, *Atmos. Chem. Phys.*, 13(18), 9321–9335, doi:10.5194/acp-13-9321-2013.
- Kumar, R., M. Naja, S. Venkataramani, and O. Wild (2010a), Variations in surface ozone at Nainital: A high-altitude site in the central Himalayas, *J. Geophys. Res.*, 115(March), 1–12, doi:10.1029/2009JD013715.
- Kumar, R., M. Naja, S. Venkataramani, and O. Wild (2010b), Variations in surface ozone at Nainital: A high-altitude site in the central Himalayas, *J. Geophys. Res. Atmos.*, 115(16), 1–12, doi:10.1029/2009JD013715.
- Kumar, R., M. Naja, G. G. Pfister, M. C. Barth, C. Wiedinmyer, and G. P. Brasseur (2012), Simulations over South Asia using the Weather Research and Forecasting model with Chemistry (WRF-Chem): Chemistry evaluation and initial results, *Geosci. Model Dev.*, 5(3), 619–648, doi:10.5194/gmd-5-619-2012.
- Lal, S., M. Naja, and B. H. Subbaraya (2000), Seasonal variations in surface ozone and its precursors over an urban site in India, *Atmos. Environ.*, 34(17), 2713–2724, doi:10.1016/S1352-2310(99)00510-5.
- Lal, S., S. Venkataramani, S. Srivastava, S. Gupta, C. Mallik, M. Naja, T. Sarangi, Y. B. Acharya, and X. Liu (2013), Transport effects on the vertical distribution of tropospheric ozone over the tropical marine regions surrounding India, *J. Geophys. Res. Atmos.*, 118(3), 1513–1524, doi:10.1002/jgrd.50180.
- Monks, P. S. et al. (2015), Tropospheric ozone and its precursors from the urban to the global scale from air quality to short-lived climate forcer, *Atmos. Chem. Phys.*, 15(15), 8889–8973, doi:10.5194/acp-15-8889-2015.
- Naja, M., S. Lal, and D. Chand (2003), Diurnal and seasonal variabilities in surface ozone at a high altitude site Mt Abu (24.6°N, 72.7°E, 1680 m asl) in India, *Atmos. Environ.*, 37(30), 4205–4215, doi:10.1016/S1352-2310(03)00565-X.
- Ohara, T., H. Akimoto, J. Kurokawa, N. Horii, K. Yamaji, X. Yan, and T. Hayasaka (2007), An Asian emission inventory of anthropogenic emission sources for the period 1980–2020, *Atmos. Chem. Phys. Discuss.*, 7(3), 6843–6902, doi:10.5194/acpd-7-6843-2007.
- Roy, S., G. Beig, and D. Jacob (2008), Seasonal distribution of ozone and its precursors over the tropical Indian region using regional chemistry-transport model, *J. Geophys. Res.*, 113(D21), D21307, doi:10.1029/2007JD009712.
- Sahu, L. K., and S. Lal (2006), Distributions of C<sub>2</sub>-C<sub>5</sub> NMHCs and related trace gases at a tropical urban site in India, *Atmos. Environ.*, 40(5), 880–891, doi:10.1016/j.atmosenv.2005.10.021.
- Srivastava, S., S. Lal, S. Venkataramani, I. Guha, and D. Bala Subrahmanyam (2012), Airborne measurements of O<sub>3</sub>, CO, CH<sub>4</sub> and NMHCs over the Bay of Bengal during winter, *Atmos. Environ.*, 59, 597–609, doi:10.1016/j.atmosenv.2012.04.054.
- Stevenson, D. S. et al. (2013), Tropospheric ozone changes, radiative forcing and attribution to emissions in the Atmospheric Chemistry and Climate Model Intercomparison Project (ACCMIP), *Atmos. Chem. Phys.*, 13(6), 3063–3085, doi:10.5194/acp-13-3063-2013.
- Surendran, D. E., S. D. Ghude, G. Beig, L. K. Emmons, C. Jena, R. Kumar, G. G. Pfister, and D. M. Chate (2015), Air quality simulation over South Asia using Hemispheric Transport of Air Pollution version-2 (HTAP-v2) emission inventory and Model for Ozone and Related chemical Tracers (MOZART-4), *Atmos. Environ.*, 122, 357–372, doi:10.1016/j.atmosenv.2015.08.023.
- Vadrevu, K. P., L. Giglio, and C. Justice (2013), Satellite based analysis of fire–carbon monoxide relationships from forest and agricultural residue burning (2003–2011), *Atmos. Environ.*, 64, 179–191, doi:10.1016/j.atmosenv.2012.09.055.
- Wang, T., H. L. A. Wong, J. Tang, A. Ding, W. S. Wu, and X. C. Zhang (2006), On the origin of surface ozone and reactive nitrogen observed at a remote mountain site in the northeastern Qinghai-Tibetan Plateau, western China, *J. Geophys. Res. Atmos.*, 111(8), 1–15, doi:10.1029/2005JD006527.
- Wang, Y., Y. Zhang, J. Hao, and M. Luo (2011), Seasonal and spatial variability of surface ozone over China: Contributions from background and domestic pollution, *Atmos. Chem. Phys.*, 11(7), 3511–3525, doi:10.5194/acp-11-3511-2011.
- van der Werf, G. R., J. T. Randerson, L. Giglio, G. J. Collatz, P. S. Kasibhatla, and a. F. Arellano (2006), Interannual variability of global biomass burning emissions from 1997 to 2004, *Atmos. Chem. Phys. Discuss.*, 6(2), 3175–3226,

doi:10.5194/acpd-6-3175-2006.

Who (2003), Health Aspects of Air Pollution with Particulate Matter , Ozone and Nitrogen Dioxide, Rep. a WHO Work. Gr. Bonn, Ger. 13–15 January 2003, (January), 98, doi:10.2105/AJPH.48.7.913.

Yadav, R., L. K. Sahu, S. N. a Jaaffrey, and G. Beig (2014),

Distributions of ozone and related trace gases at an urban site in western India, *J. Atmos. Chem.*, 71(2), 125–144, doi:10.1007/s10874-014-9286-9.

Yarragunta, Y., S. Srivastava, and D. Mitra (2017), Validation of lower tropospheric carbon monoxide inferred from MOZART model simulation over India, *Atmos. Res.*, 184, 35–47, doi:10.1016/j.atmosres.2016.09.010.